Generation of single-cycle relativistic infrared pulses at wavelengths above 20 μm from density-tailored plasmas (EP)

Xing-Long Zhu,[1,2,3,a)] (iD) Wei-Yuan Liu,[1,3] (iD) Su-Ming Weng,[1,3] (iD) Min Chen,[1,3] (iD)
Zheng-Ming Sheng,[1,2,3,4,a)] (iD) and Jie Zhang[1,2,3]

AFFILIATIONS

[1]Key Laboratory for Laser Plasmas (MOE), School of Physics and Astronomy, Shanghai Jiao Tong University,
 Shanghai 200240, China
[2]Tsung-Dao Lee Institute, Shanghai Jiao Tong University, Shanghai 200240, China
[3]Collaborative Innovation Center of IFSA, Shanghai Jiao Tong University, Shanghai 200240, China
[4]SUPA, Department of Physics, University of Strathclyde, Glasgow G4 0NG, United Kingdom

Note: This paper is a part of the Special Topic Collection on Plasma Optics.
[a)]Authors to whom correspondence should be addressed: xinglong.zhu@sjtu.edu.cn and zmsheng@sjtu.edu.cn

ABSTRACT

Ultra-intense short-pulse light sources are powerful tools for a wide range of applications. However, relativistic short-pulse lasers are normally generated in the near-infrared regime. Here, we present a promising and efficient way to generate tunable relativistic ultrashort pulses with wavelengths above 20 μm in a density-tailored plasma. In this approach, in the first stage, an intense drive laser first excites a nonlinear wake in an underdense plasma, and its photon frequency is then downshifted via phase modulation as it propagates in the plasma wake. Subsequently, in the second stage, the drive pulse enters a lower-density plasma region so that the wake has a larger plasma cavity in which longer-wavelength infrared pulses can be produced. Numerical simulations show that the resulting near-single-cycle pulses cover a broad spectral range of 10–40 μm with a conversion efficiency of ~2.1% (~34 mJ pulse energy). This enables the investigation of nonlinear infrared optics in the relativistic regime and offers new possibilities for the investigation of ultrafast phenomena and physics in strong fields.

I. INTRODUCTION

Ultrashort-duration high-energy light sources in the mid-infrared (mid-IR) spectral range play key roles in a number of areas of fundamental research, such as the scaling of strong-field interactions to mid-IR wavelengths,[1,2] high-order harmonic generation,[3] and supercontinuum generation.[4] They are also of particular interest for ultrafast molecular dynamics imaging,[5] IR spectroscopy[6] for biological and medical diagnostics, molecular fingerprinting, and the generation of optical frequency combs.[7,8] The boosting of such IR light sources to relativistic intensity will open up a new realm of research, dealing, for instance, with the generation of bright hard x-ray or even gamma-ray sources,[9] next-generation laser–plasma accelerators,[10–12] and the study of relativistic light–matter interactions in the mid-IR domain.[13] Most of these studies would benefit significantly from intense driving optical

fields with ultrashort pulse durations of a few cycles, long carrier wavelength, multi-millijoule (multi-mJ) pulse energy, and high peak intensity reaching up to the relativistic level. It is obviously an enormous challenge for current laser technology to simultaneously achieve all of these pulse parameters. So far, massive efforts have been devoted to producing few-cycle intense mid-IR pulses through various optical devices using nonlinear crystals.[14–17] However, it is still hard to expand these methods for obtaining single-cycle IR pulses at long wavelengths beyond 5 μm into the relativistic regime, since they normally suffer from optical breakdown damage and the low power-carrying capacity and limited bandwidth of optical materials.

On the other hand, plasma-based methods are of particular interest for manipulation and generation of high-intensity ultrashort laser pulses,[18–23] owing to the ability of plasmas to sustain much higher power and optical intensity without the limitations imposed by

the risk of damage. In recent years, there have been a number of proposals for the generation of intense single-cycle mid-IR pulses via photon deceleration of high-power relativistic short-pulse lasers in plasmas[24–26] or via frequency downshifting in a two-pulse laser-driven plasma optical modulator.[27] However, the central wavelengths that are produced by these methods are usually limited to a mid-IR spectral range of less than 10 μm. This can be attributed to the use of a relatively high-density plasma as a nonlinear converter, which restricts the ability of the plasma wake to form a cavity large enough to accommodate a longer-wavelength IR pulse. Hence, it remains a challenge to extend the generation of such IR pulses into the long-wavelength range beyond 20 μm with current methods.

In this work, we present a scheme to address this difficulty with the use of density-tailored plasmas as a new type of nonlinear optical medium. These plasmas have a two-stage structure, with one stage having a relatively high density for efficient pulse modulation and photon deceleration, and the other stage having moderately low density for significant frequency down-conversion to the longer-wavelength spectral domain. This has the advantage of overcoming both the restrictions imposed by limited wavelength elongation in previous plasma-based methods and the disadvantages of low damage threshold and low power amplification associated with traditional optical techniques. Finally, the drive laser pulse experiences strong frequency downshifting and continuous spectral broadening as it propagates in a plasma with such a two-stage structure, and hence it can be converted into near-single-cycle IR pulses of wavelengths above 20 μm with a few percent efficiency at relativistic intensities.

II. THEORETICAL MODEL AND NUMERICAL SIMULATION

Figure 1(a) presents a schematic illustration of how a drive laser pulse of near-IR wavelengths can be transformed into near-single-cycle IR pulses of long wavelength by using a density-tailored plasma structure. In this scheme, a relativistically intense short-pulse laser first excites a plasma wave of density disturbance to form a nonlinear wake as it propagates in an underdense plasma, as shown in Fig. 1(b). As the drive laser pulse interacts with the plasma wave, it undergoes continuous frequency downshifting via phase variation or modulation in the wake. Subsequently, the IR photons slip backward to the

central area of the wake, because they have a lower group velocity $v_g = c\left(1 - \omega_p^2/\omega_{ir}^2\right)^{1/2}$ than the drive laser photons. As soon as the created IR photons arrive at the wake center, which is near the electron-free region, they are trapped there and experience a tiny frequency shift. This configuration thus acts as an ideal optical medium for producing and sustaining intense near-single-cycle IR pulses, as shown in Fig. 1(c). To broaden such IR pulses to a new spectral range of wavelengths above 20 μm, a lower-density plasma region as a pulse stretcher is used for forming a large enough plasma cavity to generate longer-wavelength IR pulses [Fig. 1(d)].

We now discuss the physical processes involved in plasma-based optical modulation for intense IR pulse generation. As an intense laser pulse travels in a plasma, its ponderomotive force is large enough to push away almost all the plasma electrons, leaving the massive ions behind and thus creating a nonlinear plasma wave wake field. This gives rise to rapid responses in the plasma frequency $\omega_p(\xi,\tau)$ and electron density $n_e(\xi,\tau)$.[28–30] These lead to a variation in the local phase velocity of the laser pulse in the wake, which can be estimated by $dv_p/d\xi \propto \partial[n_e(\xi,\tau)]/\partial\xi$, where $\partial[n_e(\xi,\tau)]/\partial\xi$ is the plasma density gradient, thereby causing an increase or a decrease of the laser wavelength or photon frequency. Here, the local phase velocity is given by the approximate expression $v_p(\xi,\tau) \approx c[1 + \omega_p^2(\xi,\tau)/2\omega^2(\xi,\tau)]$ based on the dispersion relation $\omega^2(\xi,\tau) = \omega_p^2(\xi,\tau) + c^2k^2(\xi,\tau)$, where $\omega(\xi,\tau)$ is the instantaneous frequency of laser photons in the plasma, c is the speed of light in vacuum, $\tau = t$, and $\xi = x - ct$ is the variable in the light frame. The local change in the light wavelength within a time $d\tau$ can be expressed as $d\lambda = \Delta v_p \, d\tau$, where $\Delta v_p \approx \lambda\partial v_p/\partial\xi$ is the difference in phase velocity between two adjoining wave peaks of the light pulse, with $\frac{\partial v_p}{\partial\xi} \approx \left(\frac{c}{2n_c}\right)\left(\frac{\lambda^2}{\lambda_0^2}\right)\frac{\partial n_e(\xi,\tau)}{\partial\xi}$ (assuming $\Delta\omega \ll \omega_0$ and $\omega_p \ll \omega_0$), where $n_c = m_e\omega_0^2/4\pi e^2$ is the critical plasma density, $\omega_0 = 2\pi c/\lambda_0$ is the initial laser photon frequency, e is the elementary charge, and m_e is the electron rest mass. Therefore, one can obtain the local variation in the radiation wavelength as

$$d\lambda \approx \frac{c\lambda^3}{2\lambda_0^2 n_c} \frac{\partial n_e(\xi,\tau)}{\partial\xi} d\tau, \tag{1}$$

which can be further written in integral form as $\frac{1}{\lambda_0} - \frac{1}{\lambda^2} \approx \frac{c}{\lambda_0^2 n_c} \int_0^T \frac{\partial n_e(\xi,\tau)}{\partial\xi} d\tau$, where T is the total time of interaction of the laser
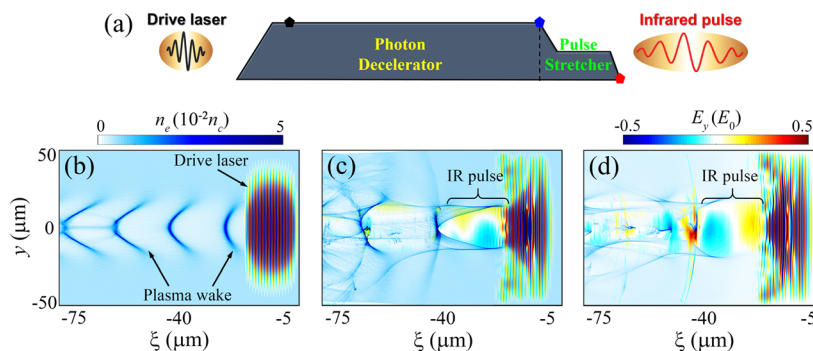

FIG. 1. (a) Schematic of the generation of long-wavelength IR pulses from a laser-driven nonlinear plasma wake in a density-tailored plasma. (b)–(d) Distributions of the transverse electric field E_y of the modulated laser pulse and the plasma wake density n_e at different positions corresponding respectively to the black dot, blue dot, and red dot in (a). Here, E_y and n_e are normalized to $E_0 \approx 3.2 \times 10^{12}$ V/m and $n_c \approx 1.1 \times 10^{21}$ cm^{-3}, respectively.

photons with plasma waves. Therefore, the resulting radiation wavelength of the light pulse in the plasma can be approximated by

$$\lambda \approx \lambda_0 \left[1 - \frac{c}{n_c} \int_0^T \frac{\partial n_e(\xi, \tau)}{\partial \xi} d\tau \right]^{-1/2}. \quad (2)$$

Equation (2) predicts that the radiation photons are frequency-redshifted in the front of the wake, where $\partial n_e(\xi, \tau)/\partial \xi > 0$, while photons are frequency-blueshifted when they arrive at the tail of the wake, where $\partial n_e(\xi, \tau)/\partial \xi < 0$, and only a very small frequency change occurs in the central area of the wake (or near the electron-free zone), where $\partial n_e(\xi, \tau)/\partial \xi \sim 0$. As a consequence, the drive laser undergoes significant wavelength widening via phase variation, and the modulated IR photons slip backward relative to the drive pulse owing to group velocity dispersion in the plasma, and they are thus potentially converted into intense long-wavelength IR pulses. This prediction is confirmed by our electromagnetic relativistic particle-in-cell (PIC) simulations detailed below.

To quantitatively investigate the underlying physics of the IR pulse generation scheme, we carry out a series of two-dimensional (2D) PIC simulations using the EPOCH code,[31] which allows self-consistent modeling of laser–plasma interactions in the relativistic regime. A simulation window moving at the speed of light along the x-axis direction is used to save computing resources, and absorbing boundary conditions are assumed for both particles and electromagnetic fields. The size of the window is $80\lambda_0(x) \times 100\lambda_0(y)$, with grid cells of 5600×600, sampled by eight macroparticles per cell. The linearly polarized laser pulse has normalized amplitude $a_0 = 2.5$ (corresponding to a peak intensity of 8.5×10^{18} W/cm^2), with a spatial profile $\exp(-r^2/r_0^2)$, pulse duration 30 fs full width at half-maximum (FWHM), $r_0 = 20\lambda_0$, wavelength $\lambda_0 = 1$ μm, oscillation frequency $\omega_0 = 2\pi c/\lambda_0$, and pulse energy 1.6 J. With the goal of generating relativistic-intensity near-single-cycle light pulses at long wavelengths as discussed earlier, the plasma structure is longitudinally tailored to form two contiguous stages that serve respectively as a photon decelerator with relatively high density and as a pulse stretcher with moderately low density, as shown in Fig. 2(a). Such a density-tailored plasma structure can be formed by inserting a blade at the entrance of the gas jet[32,33] or by using dual-stage gas jets.[34]

Figures 2(b) and 2(c) illustrate the evolutions of the electric field and the radiation wavelength of the laser pulse modulated by the wake as functions of the interaction distance in the density-tailored plasma. In the first stage, a relatively high density is employed to excite a plasma wave of large density gradient that is very beneficial for strong pulse modulation and phase variation in the plasma. It can transform the wavelength of the light pulse induced by the plasma wave to the mid-IR range as $\Delta\lambda \propto \partial n_e(\xi, \tau)/\partial \xi > 0$ [see Eq. (1)] when it resides in the region of increasing density (i.e., the front of the wake). Although this is an efficient process, the spectrum of the IR pulse that is produced is limited by the wake cavity to a central wavelength range of less than 15 μm. To overcome this bottleneck, we introduce a second stage with moderately low density as a stretcher, making the plasma wake much larger and thus enlarging the radiation pulse wavelength up to 40 μm. The resulting IR pulses fill almost the entire plasma cavity [see Fig. 1(d)] and in the long-wavelength portion have a nearly 20 μm central wavelength with a near single optical cycle and a relativistic field strength $a_{ir} = eE_{ir}/m_e c\omega_{ir} \approx 3.5$, as shown in Fig. 2. The total energy conversion efficiency from the drive laser pulse to an IR pulse of wavelength over 10 μm is about 2.1% (i.e., about 34 mJ pulse energy).

III. TUNABILITY OF IR PULSES

The radiation wavelength, peak intensity, optical cycle number, and energy conversion efficiency of the generated IR pulses are flexibly controlled by altering the plasma parameters. Here, we primarily investigate the effect of the stretcher on IR pulse generation, since the it can vary the photon frequency downshift to a much greater degree than the decelerator. We first consider the effect of the length L of the uniform-density part of the stretcher on the IR photon radiation, where L is varied from 100 to 350 μm while all other parameters are kept unchanged, as shown in Fig. 3(a). It should be noted that a suitably long plasma is advantageous to transform high-energy intense IR pulses with wavelengths beyond 20 μm. This is because it allows a long interaction distance for increasing the radiation wavelength or downshifting the photon frequency, which is consistent with our analytical model since the $\Delta\lambda \approx \frac{\lambda^3}{2\lambda_0^2 n_c} \frac{\partial n_e(\xi,\tau)}{\partial \xi} \Delta c\tau \propto \Delta L$. However, for lengths above an optimal value of $L \approx 300$ μm, the IR radiation pulse reaches saturation and gradually attenuates owing to pulse absorption and pump depletion in the plasma.
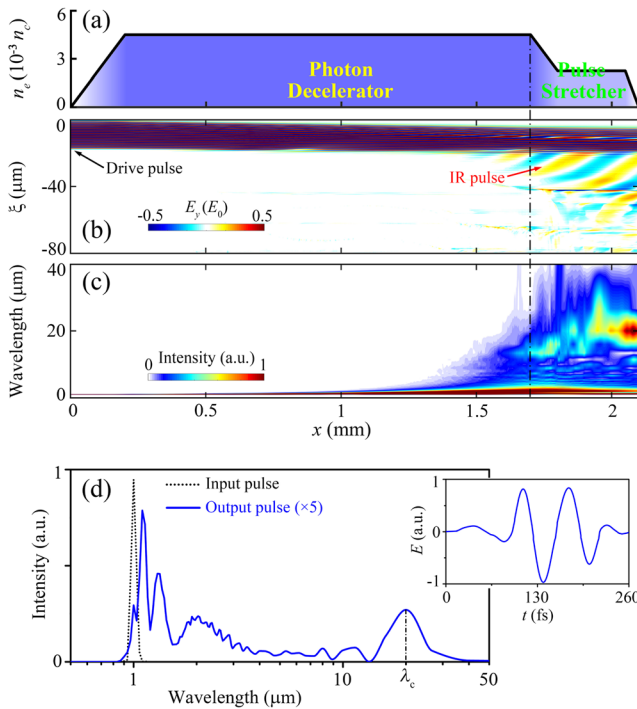

FIG. 2. (a) Density distribution of the designed plasma structure. (b) and (c) Evolutions of the transverse electric field and the radiation wavelength, respectively, of the modulated pulse in a density-tailored plasma as functions of the propagation distance x. (d) Spectral distributions of the initial laser pulse (black dotted line) and the produced IR pulse (blue solid line). The inset is a plot of the temporal waveform of the electric field of the output IR pulse in the long-wavelength part with a central wavelength of $\lambda_c \approx 20$ μm. Here, the electric field E_y of the modulated pulses is normalized to $E_0 \approx 3.2 \times 10^{12}$ V/m.
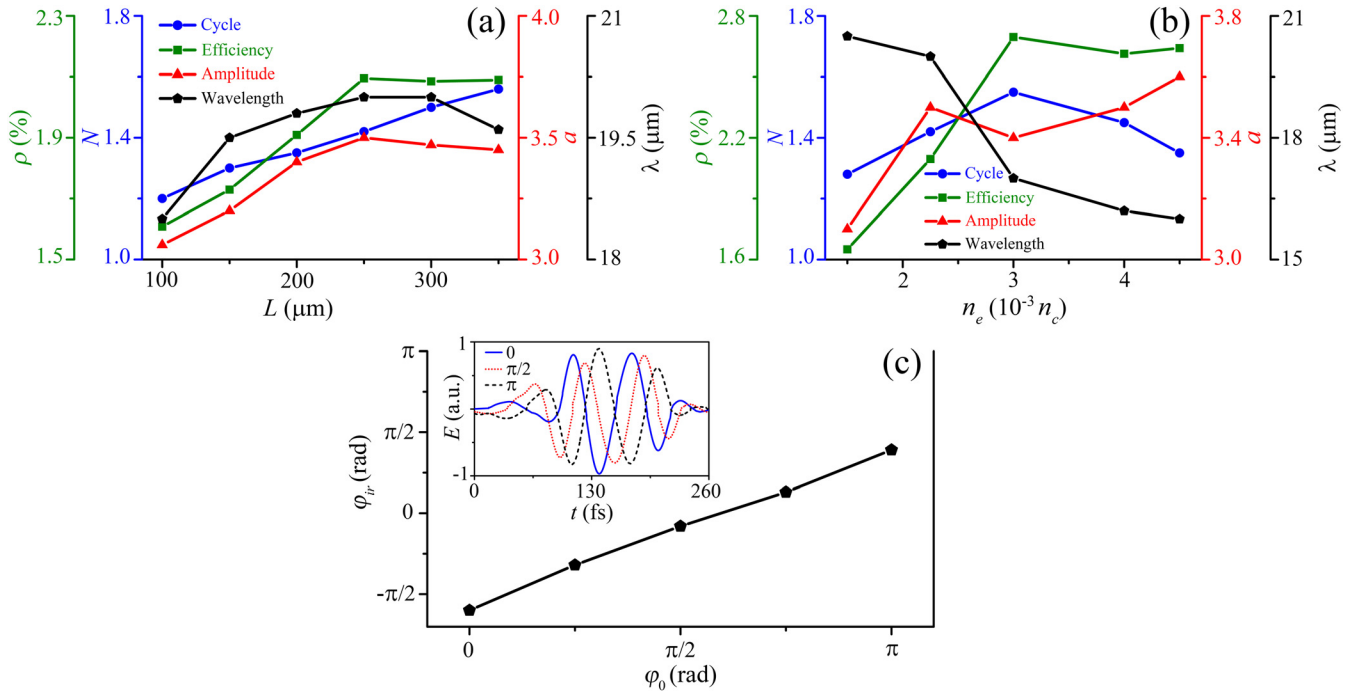
FIG. 3. (a) and (b) Energy conversion efficiency ρ, optical cycle number N, normalized amplitude a, and central wavelength λ of an IR pulse over 10 μm as functions of the length L of the uniform-density part of the stretcher and its density n_e. (c) CEP φ_{ir} of the long-wavelength IR pulse as a function of the CEP φ_0 of the drive laser pulse. The inset shows the electric field waveform of a $\lambda_c \approx 20$ μm IR pulse for three different CEPs of the initial laser pulse: $\varphi_0 = 0$ (blue solid line), $\pi/2$ (red dashed line), and π (black dashed line).

In Fig. 3(b), we investigate the influence of the density of the plasma stretcher on the IR radiation. With the increasing plasma density in the region of the stretcher, the size of the wake cavity shrinks, since the $l_w \approx 2\pi/k_p \propto \sqrt{a_0/n_e}$, and so it may not be able to contain more IR photons and thereby form longer-wavelength light pulses. This leads to a rapid decrease in the radiation wavelength of the IR pulses produced in the plasma, which is verified by our simulations. For example, the IR central wavelength is shortened to $\lambda_c \approx 16$ μm when a higher density $n_e = 4.5 \times 10^{-3} n_c$ is used. However, the plasma density should not be too low; otherwise, the density gradient of the plasma wake may be reduced so much such that it will not have enough strength to produce intense IR radiation, even though it may create a central wavelength as long as 21 μm. A lower-density plasma also requires a longer interaction distance for photon frequency downshifting [as suggested by Eq. (2)], which will cause pulse diffraction or absorption and thus weaken the generated IR pulse. In addition, a very low density can induce a steep density ramp between the decelerator and the stretcher, which may result in injection of massive plasma electrons and so consume a lot of the drive laser energy in accelerating these electrons. As a consequence, the energy conversion efficiency of the generated IR pulses will be reduced.

We now examine the robustness of this IR radiation scheme with regard to the carrier-envelope phase (CEP), which is important for light–matter interactions with few-cycle pulses.[35,36] Figure 3(c) shows the CEP of the output IR pulse as a function of the CEP of the initial laser pulse. When an intense short-pulse laser propagates in a plasma, this

gives rise to a variation in the time-dependent plasma frequency $\omega_p(\tau)$ or density $n_e(\tau)$ and thus triggers a shift in the CEP of the light pulse due to the difference between the group velocity (determining the pulse envelope) $v_g \approx c[1 - \omega_p^2(\tau)/2\omega_{ir}^2] < c$ and the phase velocity (determining the pulse phase) $v_p \approx c[1 + \omega_p^2(\tau)/2\omega_{ir}^2] > c$. The resulting shift in the carrier phase φ_{ir} of the IR pulse relative to the initial phase φ_0 of the drive laser pulse can be approximated by

$$\Delta\varphi = \varphi_{ir} - \varphi_0 \approx \int_0^T \frac{v_p - v_g}{c} \omega_{ir}(\tau) d\tau, \quad (3)$$

where $\omega_{ir}(\tau)$ is the instantaneous frequency of the IR photons produced in the plasma. By inserting $v_p \approx c[1 + \omega_p^2(\tau)/2\omega_{ir}^2]$, $v_g \approx c[1 - \omega_p^2(\tau)/2\omega_{ir}^2]$, and $\omega_p^2(\tau) = 4\pi e^2 n_e(\tau)/m_e$ into Eq. (3), we further obtain $\Delta\varphi \approx \int_0^T \frac{n_e(\tau)}{n_c} \frac{\omega_0^2}{\omega_{ir}(\tau)} d\tau$. This implies that the phase shift $\Delta\varphi$ will be determined when a specified plasma is used, because both the $\omega_{ir}(\tau)$ and $n_e(\tau)$ given by pulse modulation are fixed. This results in an almost-linear phase relationship between the IR pulse and the initial laser pulse, which is validated by our simulations, as can be seen in Fig. 3(c). Consequently, the CEP of the output IR pulse is locked and controlled by the drive pulse, which is very useful for few-cycle pulse-based applications.

IV. CONCLUSION

An efficient scheme has been proposed for generating tunable intense single-cycle IR pulses with central wavelengths above 20 μm, based on photon frequency down-conversion induced by phase

modulation in a two-stage density-tailored plasma. The operation of the scheme has been demonstrated by PIC simulations. It is found that such IR pulses can reach relativistically high intensities and pulse energies of tens of millijoules. These pulse parameters can be fully controlled by varying the plasma parameters. Moreover, the carrier envelope phase of the IR pulses is locked and controlled by that of the drive laser pulse in a specified plasma structure. The proposed scheme allows high-intensity ultrashort IR pulses to be produced over a broad spectral range of wavelengths extending up to 40 μm (reaching the THz range), which may extend the investigation of light–matter interactions into an unprecedented range of relativistic intensity and long wavelength, and with single-cycle pulses. Such powerful light sources provide an exciting new tool for exploring the frontiers of ultrafast phenomena and strong-field physics.

ACKNOWLEDGMENTS

AUTHOR DECLARATIONS

Conflict of Interest

The authors have no conflicts to disclose.

Author Contributions

X.-L.Z. and W.-Y.L. contributed equally to this work.

DATA AVAILABILITY

The data that support the findings of this study are available from the corresponding author upon request.

REFERENCES

[1]P. Colosimo, G. Doumy, C. I. Blaga, J. Wheeler, C. Hauri, F. Catoire, J. Tate, R. Chirla, A. M. March, G. G. Paulus, H. G. Muller, P. Agostini, and L. F. DiMauro, "Scaling strong-field interactions towards the classical limit," Nat. Phys. **4**, 386 (2008).

[2]B. Wolter, M. G. Pullen, M. Baudisch, M. Sclafani, M. Hemmer, A. Senftleben, C. D. Schröter, J. Ullrich, R. Moshammer, and J. Biegert, "Strong-field physics with mid-IR fields," Phys. Rev. X **5**, 021034 (2015).

[3]T. Popmintchev, M.-C. Chen, D. Popmintchev, P. Arpin, S. Brown, S. Ališauskas, G. Andriukaitis, T. Balčiunas, O. D. Mücke, A. Pugzlys, A. Baltuška, B. Shim, S. E. Schrauth, A. Gaeta, C. Hernández-García, L. Plaja, A. Becker, A. Jaron-Becker, M. M. Murnane, and H. C. Kapteyn, "Bright coherent ultrahigh harmonics in the keV x-ray regime from mid-infrared femtosecond lasers," Science **336**, 1287 (2012).

[4]F. Silva, D. R. Austin, A. Thai, M. Baudisch, M. Hemmer, D. Faccio, A. Couairon, and J. Biegert, "Multi-octave supercontinuum generation from mid-infrared filamentation in a bulk crystal," Nat. Commun. **3**, 807 (2012).

[5]C. I. Blaga, J. Xu, A. D. DiChiara, E. Sistrunk, K. Zhang, P. Agostini, T. A. Miller, L. F. DiMauro, and C. D. Lin, "Imaging ultrafast molecular dynamics with laser-induced electron diffraction," Nature **483**, 194 (2012).

[6]I. Pupeza, M. Huber, M. Trubetskov, W. Schweinberger, S. A. Hussain, C. Hofer, K. Fritsch, M. Poetzlberger, L. Vamos, E. Fill, T. Amotchkina, K. V. Kepesidis, A. Apolonski, N. Karpowicz, V. Pervak, O. Pronin, F. Fleischmann, A. Azzeer, M. Žigman, and F. Krausz, "Field-resolved infrared spectroscopy of biological systems," Nature **577**, 52 (2020).

[7]C. R. Petersen, U. Møller, I. Kubat, B. Zhou, S. Dupont, J. Ramsay, T. Benson, S. Sujecki, N. Abdel-Moneim, Z. Tang, D. Furniss, A. Seddon, and O. Bang, "Mid-infrared supercontinuum covering the 1.4–13.3 μm molecular fingerprint region using ultra-high NA chalcogenide step-index fibre," Nat. Photonics **8**, 830 (2014).

[8]A. Schliesser, N. Picqué, and T. W. Hänsch, "Mid-infrared frequency combs," Nat. Photonics **6**, 440 (2012).

[9]J. Weisshaupt, V. Juvé, M. Holtz, S. Ku, M. Woerner, T. Elsaesser, S. Ališauskas, A. Pugžlys, and A. Baltuška, "High-brightness table-top hard X-ray source driven by sub-100-femtosecond mid-infrared pulses," Nat. Photonics **8**, 927 (2014).

[10]T. Tajima and J. M. Dawson, "Laser electron accelerator," Phys. Rev. Lett. **43**, 267 (1979).

[11]I. V. Pogorelsky, I. Babzien, I. Ben-Zvi, M. N. Polyanskiy, J. Skaritka, O. Tresca, N. P. Dover, Z. Najmudin, W. Lu, N. Cook, A. Ting, and Y.-H. Chen, "Extending laser plasma accelerators into the mid-IR spectral domain with a next-generation ultra-fast CO_2 laser," Plasma Phys. Controlled Fusion **58**, 034003 (2016).

[12]X.-L. Zhu, W.-Y. Liu, M. Chen, S.-M. Weng, F. He, R. Assmann, Z.-M. Sheng, and J. Zhang, "Generation of 100-MeV attosecond electron bunches with terawatt few-cycle laser pulses," Phys. Rev. Appl. **15**, 044039 (2021).

[13]Z. Samsonova, S. Höfer, V. Kaymak, S. Ališauskas, V. Shumakova, A. Pugžlys, A. Baltuška, T. Siefke, S. Kroker, A. Pukhov, O. Rosmej, I. Uschmann, C. Spielmann, and D. Kartashov, "Relativistic interaction of long-wavelength ultrashort laser pulses with nanowires," Phys. Rev. X **9**, 021029 (2019).

[14]I. Pupeza, D. Sánchez, J. Zhang, N. Lilienfein, M. Seidel, N. Karpowicz, T. Paasch-Colberg, I. Znakovskaya, M. Pescher, W. Schweinberger, V. Pervak, E. Fill, O. Pronin, Z. Wei, F. Krausz, A. Apolonski, and J. Biegert, "High-power sub-two-cycle mid-infrared pulses at 100 MHz repetition rate," Nat. Photonics **9**, 721 (2015).

[15]V. Shumakova, P. Malevich, S. Ališauskas, A. Voronin, A. M. Zheltikov, D. Faccio, D. Kartashov, A. Baltuška, and A. Pugžlys, "Multi-millijoule few-cycle mid-infrared pulses through nonlinear self-compression in bulk," Nat. Commun. **7**, 12877 (2016).

[16]H. Liang, P. Krogen, Z. Wang, H. Park, T. Kroh, K. Zawilski, P. Schunemann, J. Moses, L. F. DiMauro, F. X. Kärtner, and K.-H. Hong, "High-energy mid-infrared sub-cycle pulse synthesis from a parametric amplifier," Nat. Commun. **8**, 141 (2017).

[17]P. Krogen, H. Suchowski, H. Liang, N. Flemens, K.-H. Hong, F. X. Kärtner, and J. Moses, "Generation and multi-octave shaping of mid-infrared intense single-cycle pulses," Nat. Photonics **11**, 222 (2017).

[18]C. Thaury, F. Quéré, J.-P. Geindre, A. Levy, T. Ceccotti, P. Monot, M. Bougeard, F. Réau, P. d'Oliveira, P. Audebert, R. Marjoribanks, and P. Martin, "Plasma mirrors for ultrahigh-intensity optics," Nat. Phys. **3**, 424 (2007).

[19]L.-L. Yu, Y. Zhao, L.-J. Qian, M. Chen, S.-M. Weng, Z.-M. Sheng, D. A. Jaroszynski, W. B. Mori, and J. Zhang, "Plasma optical modulators for intense lasers," Nat. Commun. **7**, 11893 (2016).

[20]A. Leblanc, A. Denoeud, L. Chopineau, G. Mennerat, P. Martin, and F. Quéré, "Plasma holograms for ultrahigh-intensity optics," Nat. Phys. **13**, 440 (2017).

[21]S. Weng, Q. Zhao, Z. Sheng, W. Yu, S. Luan, M. Chen, L. Yu, M. Murakami, W. B. Mori, and J. Zhang, "Extreme case of Faraday effect: Magnetic splitting of ultrashort laser pulses in plasmas," Optica **4**, 1086 (2017).

[22]M. Zeng, A. Martinez de la Ossa, K. Poder, and J. Osterhoff, "Plasma eyepieces for petawatt class lasers," Phys. Plasmas **27**, 023109 (2020).

[23]L. Chopineau, A. Denoeud, A. Leblanc, E. Porat, P. Martin, H. Vincenti, and F. Quéré, "Spatio-temporal characterization of attosecond pulses from plasma mirrors," Nat. Phys. **17**, 968 (2021).

[24]F. S. Tsung, C. Ren, L. O. Silva, W. B. Mori, and T. Katsouleas, "Generation of ultra-intense single-cycle laser pulses by using photon deceleration," Proc. Natl. Acad. Sci. U. S. A. **99**, 29 (2002).

[25]Z. Nie, C.-H. Pai, J. Hua, C. Zhang, Y. Wu, Y. Wan, F. Li, J. Zhang, Z. Cheng, Q. Su, S. Liu, Y. Ma, X. Ning, Y. He, W. Lu, H.-H. Chu, J. Wang, W. B. Mori, and C. Joshi, "Relativistic single-cycle tunable infrared pulses generated from a tailored plasma density structure," Nat. Photonics **12**, 489 (2018).

[26]X.-L. Zhu, M. Chen, S.-M. Weng, P. McKenna, Z.-M. Sheng, and J. Zhang, "Single-cycle terawatt twisted-light pulses at midinfrared wavelengths above 10 μm," Phys. Rev. Appl. **12**, 054024 (2019).

[27]X.-L. Zhu, S.-M. Weng, M. Chen, Z.-M. Sheng, and J. Zhang, "Efficient generation of relativistic near-single-cycle mid-infrared pulses in plasmas," Light: Sci. Appl. **9**, 46 (2020).

[28]S. C. Wilks, J. M. Dawson, W. B. Mori, T. Katsouleas, and M. E. Jones, "Photon accelerator," Phys. Rev. Lett. **62**, 2600 (1989).

[29]P. Sprangle, E. Esarey, and A. Ting, "Nonlinear theory of intense laser-plasma interactions," Phys. Rev. Lett. **64**, 2011 (1990).

[30]Z.-M. Sheng, J.-X. Ma, Z.-Z. Xu, and W. Yu, "Effect of an electron plasma wave on the propagation of an ultrashort laser pulse," J. Opt. Soc. Am. B **10**, 122 (1993).

[31]T. D. Arber, K. Bennett, C. S. Brady, A. Lawrence-Douglas, M. G. Ramsay, N. J. Sircombe, P. Gillies, R. G. Evans, H. Schmitz, A. R. Bell, and C. P. Ridgers, "Contemporary particle-in-cell approach to laser-plasma modelling," Plasma Phys. Controlled Fusion **57**, 113001 (2015).

[32]A. Buck, J. Wenz, J. Xu, K. Khrennikov, K. Schmid, M. Heigoldt, J. M. Mikhailova, M. Geissler, B. Shen, F. Krausz, S. Karsch, and L. Veisz, "Shock-front injector for high-quality laser-plasma acceleration," Phys. Rev. Lett. **110**, 185006 (2013).

[33]E. Guillaume, A. Döpp, C. Thaury, K. Ta Phuoc, A. Lifschitz, G. Grittani, J.-P. Goddet, A. Tafzi, S. W. Chou, L. Veisz, and V. Malka, "Electron rephasing in a laser-wakefield accelerator," Phys. Rev. Lett. **115**, 155002 (2015).

[34]W. T. Wang, W. T. Li, J. S. Liu, Z. J. Zhang, R. Qi, C. H. Yu, J. Q. Liu, M. Fang, Z. Y. Qin, C. Wang, Y. Xu, F. X. Wu, Y. X. Leng, R. X. Li, and Z. Z. Xu, "High-brightness high-energy electron beams from a laser wakefield accelerator via energy chirp control," Phys. Rev. Lett. **117**, 124801 (2016).

[35]T. Wittmann, B. Horvath, W. Helml, M. G. Schätzel, X. Gu, A. L. Cavalieri, G. G. Paulus, and R. Kienberger, "Single-shot carrier–envelope phase measurement of few-cycle laser pulses," Nat. Phys. **5**, 357 (2009).

[36]N. Ishii, K. Kaneshima, K. Kitano, T. Kanai, S. Watanabe, and J. Itatani, "Carrier-envelope phase-dependent high harmonic generation in the water window using few-cycle infrared pulses," Nat. Commun. **5**, 3331 (2014).